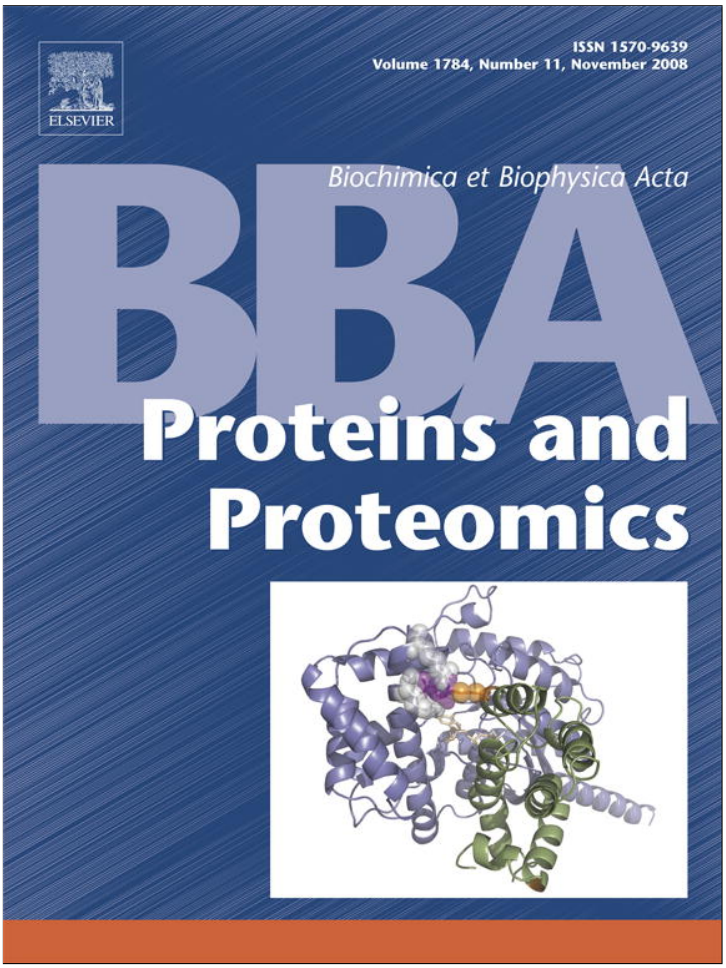

Biochimica et Biophysica Acta 1784 (2008) 1617–1624

Contents lists available at ScienceDirect

Biochimica et Biophysica Acta

journal homepage: www.elsevier.com/locate/bbapap

Reversibility and "pH–*T* phase diagrams" of *Rapana venosa* hemocyanin and its structural subunits

Alexandar Dolashki [a], Lyudmila Velkova [b], Boris Atanasov [b,*], Wolfgang Voelter [a], Stefan Stevanovic [c], Heinz Schwarz [d], Paolo Di Muro [e], Pavlina Dolashka-Angelova [b,*]

[a] *Interfacultary Institute of Biochemistry, University of Tübingen, Hoppe-Seyler-Straße 4, D-72076 Tübingen, Germany*
[b] *Institute of Organic Chemistry, Bulgarian Academy of Sciences, G. Bonchev 9, Sofia 1113, Bulgaria*
[c] *Department of Immunology, Institute for Cell Biology, University of Tübingen, Auf der Morgenstelle 15, D-72076 Tübingen, Germany*
[d] *Max-Planck-Institut fuer Entwicklungsbiologie, Spemannstr. 35, D-72076 Tuebingen, Germany*
[e] *Department of Biology, University of Padova, via G. Colombo 3, 35131 Padova, Italy*

ARTICLE INFO

Article history:
Received 5 March 2008
Received in revised form 3 June 2008
Accepted 5 June 2008
Available online 14 June 2008

Keywords:
Electron microscopy
Rapana venosa hemocyanin
pH stability
Transition curves
Circular dichroism

ABSTRACT

We have studied the stability and reassociation behaviour of native molecules of *Rapana venosa* hemocyanin and its two subunits, termed RvH1 and RvH2. In the presence of different concentrations of Ca^{2+} and Mg^{2+} ions and pH values, the subunits differ not only in their reassociation behaviour, but also in their formation of helical tubules and multidecamers. RvH1 revealed a greater stability at higher pH values compared to RvH2. Overall, the stability of reassociated RvH and its structural subunits was found to be pH-dependent. The increasing stability of native Hc and its subunits, shown by pH-induced CD transitions (acid and alkaline denaturation), can be explained with the formation of quaternary structure. The absence of a Cotton effect at temperatures 20–40 °C in the pH-transition curves of RvH2 indicates that this subunit is stabilized by additional "factors", e.g.: non-ionic/hydrophobic stabilization and interactions of carbohydrate moieties. A similar behaviour was observed for the T-transition curves in a wide pH interval for RvH and its structural subunits. At higher temperatures, many of the secondary structural elements are preserved especially at neutral pH, even at extreme high temperatures above 90 °C the protein structures resemble a "globule state".

1. Introduction

In the hemolymph of many arthropodan and molluscan species oxygen is transported by large copper-containing respiratory proteins, termed hemocyanins [1,2]. These proteins bind oxygen reversible at a binuclear active site and transport it to the tissues. In spite of their similar function, the quaternary structure and arrangement of subunits and their properties vary considerably in different species. The basic quaternary structure of molluscan hemocyanin is a ring-like decameric homo-oligomer, assembled from 10 copies of a ~350- to 400 kDa subunit. In gastropods and bivalves the typical quaternary structure for native hemocyanin is a cylindrical didecamer, formed by face-to-face assembly of two decamers [2]. Several gastropodan hemocyanins are heterogeneous in that they consist of two immunologically distinct subunit isoforms that are differentially expressed [3]. The subunit of gastropod hemocyanin is a ~400 kDa polypeptide folded into seven or eight different covalently linked globular functional units (FUs) of M_r ~50 kDa, termed FU-a to FU-h (from the N- to the C-terminus). Each FU contains two copper atoms which reversibly bind one dioxygen molecule [4]. Hemocyanin of the gastropods *Megathura crenulata* [5], *Haliotis tuberculata* [6], and *Rapana venosa* [7] has two distinct native homodecameric forms each containing one of the two subunit isoforms.

Extensive experimental studies using different dissociation and reassociation conditions of native molluscan hemocyanins (e.g. removal of divalent cations) [8–11], pH changes or the addition of denaturing agents [12] have helped to elucidate its subunit composition and structure.

In this context we have studied the biochemical properties of total (native) RvH and its structural subunits RvH1 and RvH2 over a broad range of temperature and pH. Physicochemical as well as functional aspects of RvH hemocyanin have already been studied, which provide a firm basis for our present investigation. The association–dissociation properties of molluscan and arthropod Hcs [13–17], together with the conformational stability of Hcs under various physical conditions (i.e. temperature) [11,17,18] and/or chemical agents [12,16,17] have been studied. However, such studies may be complicated by the fact it may

Abbreviations: TEM, transmission electron microscopy; Hc, hemocyanin; SB, stabilizing buffer; RvH, *Rapana venosa* Hc; RvH1 and RvH2, subunit isoforms 1 and 2 of *Rapana venosa* Hc

* Corresponding authors. Institute of Organic Chemistry, Bulgarian Academy of Sciences, Acad. G. Bonchev Street, bl. 9, 1113 Sofia, Bulgaria. Tel.: +359 2 9606163/123; fax: +359 2 8700225.
E-mail addresses: boris@orgchm.bas.bg (B. Atanasov), pda54@yahoo.com (P. Dolashka-Angelova).

1570-9639/$ – see front matter © 2008 Elsevier B.V. All rights reserved.
doi:10.1016/j.bbapap.2008.06.004

be difficult to distinguish between the effects on the quaternary structure of the oligomeric protein (i.e. initial dissociation) and those on the tertiary and secondary structure (i.e. subunit unfolding), depending upon the dissociation conditions.

R. venosa (rename by *Rapana thomasiana*) is a prosobranch gastropod, collected from the Black Sea. Electron micrographs of purified native hemocyanin showed a homogenous preparation of didecamers [11]. Data on this hemocyanin have been published concerning amino acid composition, carbohydrate content, dissociation, and reassociation behaviour and spectroscopic properties [7,11,12]. The two types of subunits identified in the hemolymph of these animals, now termed RHSS1 and RHSS2 [19,20], have molecular masses of ~420 kDa and ~450 kDa, respectively.

Hydrodynamic parameters of *Rapana* hemocyanin were determined by dynamic light scattering [21], while the thermal stability of RvH was studied by different scanning calorimetry [22]. Irreversibility of the thermal denaturation was also observed in DSC measurements of the Hcs from lobster *Palinurus vulgaris* [23] and tarantula *Eurypelma californicum* [24] and is a common observation for high molecular mass hemocyanin molecules.

The main aim of this study is to determine the reversibility/irreversibility and association–dissociation behaviour of RvH, its structural subunits with respect to pH and temperature using circular dichroism (CD). The narrow range over which the system is reversible has been determined using two independent ways of denaturation and the corresponding thermodynamic parameters were calculated.

2. Materials and methods

2.1. Isolation of R. venosa hemocyanin

Native Hc, containing a mixture of the two subunits, was purified from the hemolymph of *R. venosa* (*R. thomasiana*) Hc as described previously [11]. The two isoforms RvH1 and RvH2 were eluted as dissociated subunits in a purified form from an ion-exchange chromatography column Resource Q 6 ml in 50 mM Tris/HCl buffer, pH 8.2, with a 0–0.5 M NaCl gradient [11].

2.2. Electron microscopy

The dissociation and reassociation behaviours of total RvH and its two subunits RvH1 and RvH2 were studied by transmission electron microscopy (TEM). For the TEM studies, samples of native RvH and purified subunits RvH1 and RvH2 were dialyzed by overnight at 4 °C against 0.13 M Glycine/NaOH buffer. The reassociation behaviour of the dissociated molecules was studied in 50 mM Tris/HCl, 150 mM NaCl, stabilizing buffer (SB), pH 7.0, containing two different concentrations of $CaCl_2$ and $MgCl_2$ (10 and 100 mM, respectively).

The stability of the reassociated multi-decameric forms of subunits RvH1 and RvH2 was investigated after dialysis of the proteins against the same buffer, but with different pH values (pH 7.0, 8.6, 9.2 and 9.6). Studies of EM specimens were performed using a Philips CM10 transmission electron microscope with a 30 mm objective aperture. Samples were adsorbed for 60 s to glow-discharged pistoform/carbon-coated support films, washed three times with droplets of distilled water to remove buffer salts and then negatively stained with 1% w/v uranyl acetate. Electron micrographs were routinely recorded at an instrumental magnification of ×52,000.

2.3. CD measurements

Circular dichroism (CD) spectra were recorded in a J-720 spectropolarimeter (Jasco, Tokyo, Japan). Cylindrical temperature-controlled quartz cells with a path length of 10 mm were used in all experiments. CD spectra were recorded in the range between 200 and 250 nm at 0.2 nm intervals with a bandwidth of 1 nm, a scan speed of 50 nm/min, and a time constant of 8.0 s. Protein solutions in 20 mM Tris/HCl, 10 mM $CaCl_2$ buffer with different pH values (from 1.5 to 12.0) were thermostatically controlled using a NESLAB thermostat model RTE-110, connected to a digital programming controller and a thermocouple placed inside the optical cell. Temperature denaturation studies for the samples at different pH (from 1.5 to 12.0) were measured after 20 min incubation, from 15 up to 95 °C the $[\theta]_{222}$ values were recorded in intervals of 5 ± 0.2 °C. Thereafter, temperature was decreased at the same rate down to 25 °C. The thermal equilibrium of samples was confirmed at each temperature by the constancy of their ellipticity. Each experimental spectrum was obtained by averaging two or three separate scans and was corrected for baseline, recorded with buffer as blank. The CD spectrum of a protein can be considered as the sum of the CD spectra of each secondary structure component of the protein.

2.4. Evaluation of effective thermodynamic functions and determination of cross-overlapped CD data

CD spectra of standardized hemocyanin solutions (see above) were recorded from 190 to 240 nm in a wide interval of pH (2–12, with ~0.5 pH unit steps) and temperature (20–85 °C with 5 °C steps). More precisely, the extreme values at 222 nm were digitalized and recalculated in $[\theta]_{222}$ (deg cm^2 $dmol^{-1}$) units. Two independent sets of experimental data – $[\theta]_{222}$ as a function of T °C for 14–15 samples at different pH and $[\theta]_{222}$ as a function of pH for 14–15 samples at different T °C – were collected for each of the three above described proteins (native RvH and the purified subunits RvH1 and RvH2). For each protein the experimental matrix $[\theta]_{exp}(T)$ was converted to the calculated $[\theta]_{cal}$(pH) and the matrix $[\theta]_{exp}$(pH) — to the $[\theta]_{cal}(T)$. The total reversibility of the system suggests independence of the terminal states from the path(s) of realization. Thus, if our system is reversible, then $[\theta]_{cal}(T)$ curves must be identical as $[\theta]_{exp}(T)$ curves and the $[\theta]_{cal}$(pH) curves will be identical for $[\theta]_{exp}$(pH) curves. To prove this strong requirement of reversibility we have extracted each pair of curves with the same (T, pH) signatures and plotted these as $\Delta[\theta](T)$ and $\Delta[\theta]$(pH). The relative percentage of $\Delta[\theta]$ with steps of 4% was used to construct "T–pH phase diagrams" for each of the three proteins within 80–100% reversibility.

2.5. Estimation of the effective "melting temperatures" (T_m) and the "T_m–pH phase diagram"

From averaged $[\theta]_{exp}(T)$ curves, neglecting the complexity of the averaged curve and an oversimplified assumption for the "two-state" (N↔D) mechanism (crude "zero approximation"), we estimate T_m as the temperature of half-denaturation for each set of each of the three proteins. The results are plotted as T_m (pH). In this case, T_m is used as integral characteristics of a structure containing different proteins (*ie*, two different subunits and their "polymeric" complex) with the expectation that there will be T–pH-dependent changes in quaternary structures. Our van't Hoff's analysis of these data was made using plots of $\log K_{obs}/R$ *vs* $1/T$ and calculating

$$\Delta G_{vh} = RT \ln K_{obs} = RT[Y/(1-Y)]$$

where Y is the relative ($0<Y<1$) change of $[\theta]_{exp}$ as a function of the temperature (in K). The results obtained are shown in Table 1.

2.6. Deconvolution of $[\theta]_{exp}$, (T,pH) curves and evaluation of $T_{m,i}$ and $pH_{d,i}$

Firstly, the starting and finishing "linear" parts of the curves are T, pH-dependent. Their slopes for $[\theta]_{exp,i}(T)$ were graphically evaluated

as B_N and B_D for different pHs. Using reversibility, T–pH intervals ($0.85 < \mathrm{Rev} < 1$) and "mirror image" curves

$$\Delta G_{vh} = -RT \ln K_{obs} = -RT[Y/(1-Y)] \text{ and } \log K_{obs}/R \text{ vs } 1/T$$

— all lines with two slopes B_N and B_D.

From B(pH) at the extreme pH – dCD/dT(pH) – analog to Z(pH) curve

From apparent "cross-points" – "the process separator" – $\alpha = \Delta CD_1/\Delta CD_t < 1$

By fitting to non-linear two-step T transition (Swint and Robertson 1993) using the following equation:

$$\begin{aligned} CD(T) = \alpha\{(CD_N + B_N T) + (CD_I + B_N T)[\exp(\Delta H_I/R(1/T_{m,1} - 1/T))] \\ : [1 + \exp(\Delta H_I/R(1/T_{m,1} - 1/T)] + (1-\alpha)\{(CD_I + B_D T) \\ + (CD_D + B_D T)[\exp(\Delta H_2/R(1/T_{m,2} - 1/T))] \\ : [1 + \exp(\Delta H_2/R(1/T_{m,2} - 1/T))] \end{aligned}$$

where known/experimental found parameters are: CD_N, , CD_D, $B[Z$(pH)] and CD(pH), but α or CD_I, $T_{m,1}$ and $T_{m,2}$, and ΔH_1 and ΔH_2 are under estimation [25].

By numerical derivation of each $CD(T)_{pH}$ curve and the integral split into two Gaussians with appropriate sites ($T_{m,1}$, $T_{m,2}$) and width (ΔT_1, ΔT_2) — from the latter, the effective (van't Hoff's) enthalpy of transitions were calculated from ($\Delta H_{vh} \equiv \Delta H_{eff}$)

$$\Delta H_{eff} = 4R(273 + T_{m,n})^2/1000 \cdot \Delta T_n \text{ (kcal/mol)}$$

where $T_{m,n}$ and ΔT_n are "melting" temperatures and half-width of the n-th transition ($n = 1, 2$) [26].

2.7. Calculation of thermodynamic functions (ΔC_p, ΔH, ΔS and ΔG of transitions)

The principal equations used in determination of thermodynamic functions at standard conditions ($T_o = 298$ K and $\Delta C_p = \partial \Delta H_{m,i}/\partial T_{m,I}$) [27] were:

$$\Delta H_i = \Delta H_{m,i} - \Delta C_p(T_{m,i} - T_o) \quad \text{(kcal/mol)}$$

$$\Delta S_i = \Delta H_{m,i}/T_{m,i} - \Delta C_p \cdot \ln(T_{m,i} - T_o) \quad \text{(cal/mol} \cdot \text{grad)}$$

$$\Delta G_i = \Delta H_{m,i}[(1 - T_{m,i} - T_o)] - \Delta C_p(T_{m,i} - T_o) - T \cdot \ln(T_{m,i} - T_o)) \quad \text{(kcal/mol)}$$

3. Results

3.1. Stability and the reassociation behaviour of native RvH molecules

Native Hc was purified from the hemolymph of *R. venosa* Hc and the native RvH and two structural subunits RvH1 and RvH2 were

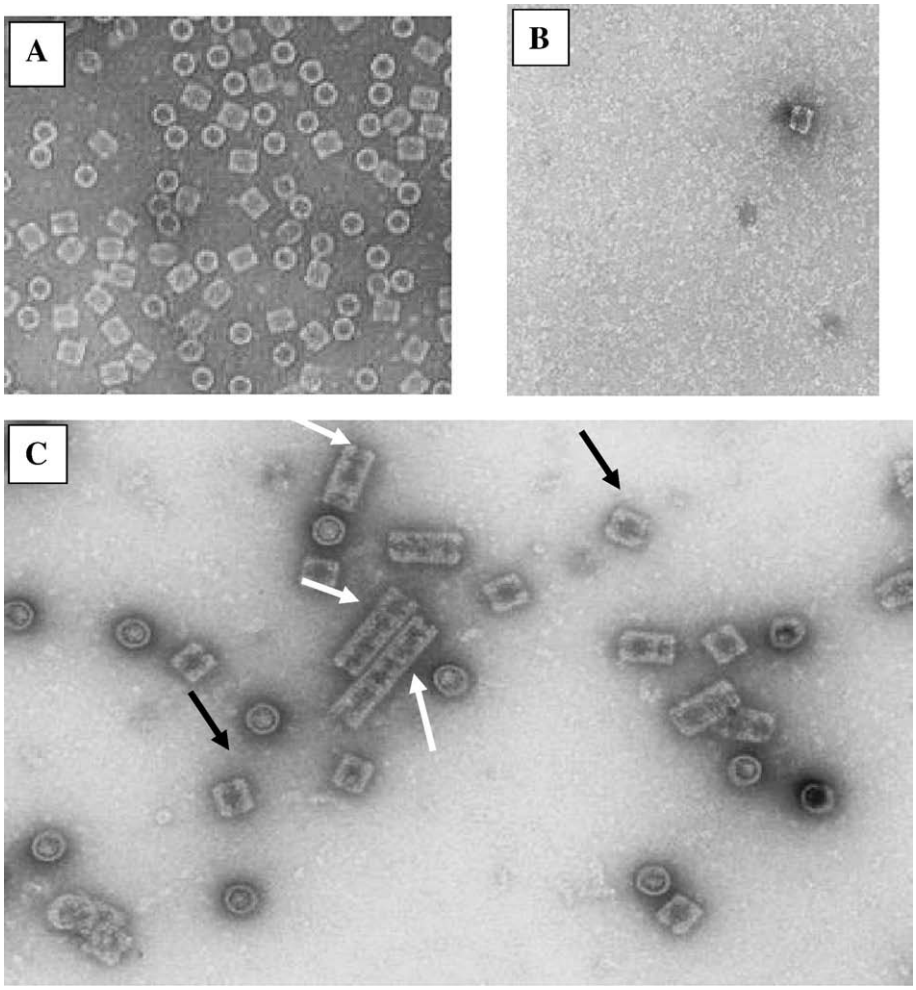

Fig. 1. Electron micrographs of *R. venosa* hemocyanin. (A) Native Hc (RvH) in 50 mM Tris/HCl buffer, pH 7.0, containing 20 mM $CaCl_2$ and 5 mM $MgCl_2$; (B) dissociated native RvH in 0.13 M Gly/NaOH buffer at pH 9.6; (C) reassociated native RvH after dialysis for 2 days against SB, pH 7.0, containing 50 mM $CaCl_2$ and $MgCl_2$ (reassociation is almost complete). By increasing the concentrations of both divalent ions, Ca^{2+} and Mg^{2+}, to 100 mM, the reassociation is increased, and not only didecamers (black arrowheads), but also multidecamers (white arrowheads) are produced. Negative staining with 1% uranyl acetate was performed as described in Materials and methods. The scale bars indicate 100 nm.

isolated as described previously [11]. Stability and their reassociation behaviour were studied in the presence of different concentrations of Ca^{2+} and Mg^{2+} ions and pH using electron microscopy. The ionic manipulation of the samples was achieved by adding calcium and magnesium ions to the dissociated samples by dialysis and the reassociation behaviour was studied after 1 to 3 days, or 1 week by TEM.

Fig. 1A shows that the native RvH molecules appear as a hollow cylindrical didecameric structure in 50 mM Tris/HCl buffer, pH 7.0, containing 20 mM $CaCl_2$ and 5 mM $MgCl_2$ (SB). After 24-h dialysis against 0.13 M Gly/NaOH buffer, pH 9.6, the native RvH is almost fully dissociated into its structural subunits RvH1 and RvH2 (Fig. 1B).

As shown in Fig. 1C, after reassociation of the fully dissociated protein within three days in SB (pH 7.0) containing 20 or 50 mM $CaCl_2$ and $MgCl_2$, respectively, the sample is structurally more heterogeneous than the native protein. Some subunits are still present, didecamers (black arrowheads) and also multidecamers (white arrowheads). The reassociation was considered to be complete after three days of dialysis in SB, containing 100 mM $CaCl_2$ and $MgCl_2$ (Table 1).

3.2. Stability and the reassociation behaviour of the structural subunits RvH1 and RvH2

The dissociated RvH1 reassociated after a 3 day dialysis in 50 mM Tris/HCl buffer (pH 9.6) in 50 mM Tris/HCl buffer (pH 7.0) containing 50 or 100 mM $CaCl_2$ and $MgCl_2$, as twisted ribbon helical tubules, partially annealed (Fig. 2A, B). The tubular polymers of RvH1 are of significant smaller diameter than the native multidecamers of KLH2 (ca. 25 versus 33 nm) [29].

The reassociation product of dissociated RvH2 is shown in Fig. 3. After reassociation of the dissociated RvH2 for three days against 50 mM Tris buffer, containing 50 mM $CaCl_2$ and $MgCl_2$ (pH 7.0), didecamers, short multidecamers and some subunits were formed (Fig. 3). Also, in SB containing 100 mM $CaCl_2$ and $MgCl_2$ (pH 7.0), short multidecamers, tubules and didecamers are present. The comparison of 50 and 100 mM is hardly relevant.

The stability of the reassociated structural subunits was found to be pH-dependent. After dialysis of reassociated RvH1 for 1–3 days against 50 mM Tris/HCl buffer, pH 8.6, containing 100 mM $CaCl_2$ and $MgCl_2$, the length of the RvH1 helical tubules was shorter.

By increasing the pH of the SB, RvH2 multidecamers are pH-dependent as those of RvH1 [11]. In the presence of high concentrations (100 mM) of Ca^{2+} and Mg^{2+} ions and increase of pH of SB to 9.6, short multidecamers, and mainly didecameric RvH2 forms and some subunits are detected [11].

3.3. Influence of temperature on circular dichroism at different pH values

All data collected from the CD-spectra have the values of $[\theta]_{222}$, which manifested the structural state of the groups of the main chain. As the molecular unit here is accepted as the subunit with an averaged molecular mass of 420–450 kDa, the estimated value of 1 deg cm^2 $dmol^{-1}$ thus corresponds to $[m]'_{222}$ for a peptide unit. Also, it must be noted that changes of $[\theta]_{222}$ (especially small ones) are not related simply to changes in polypeptide helicity, but more generally to changes in interactions and orientations of protein peptide dipoles.

Three sets of data were obtained for native RvH and for each of its two subunits RvH1 and RvH2 (see Fig. 4A, B, C). An initial feature is the presence of T-induced changes within a wide temperature interval (25–85 °C). Secondly, specificity is irreversibility to common “end states” with a relatively similar disordered structure. The latter is especially characteristic for the native Hc RvH. The amplitude $\Delta[\theta]_N - \Delta[\theta]_D$ for curves at different pH is slightly decreased on moving to extreme pH values. For some of

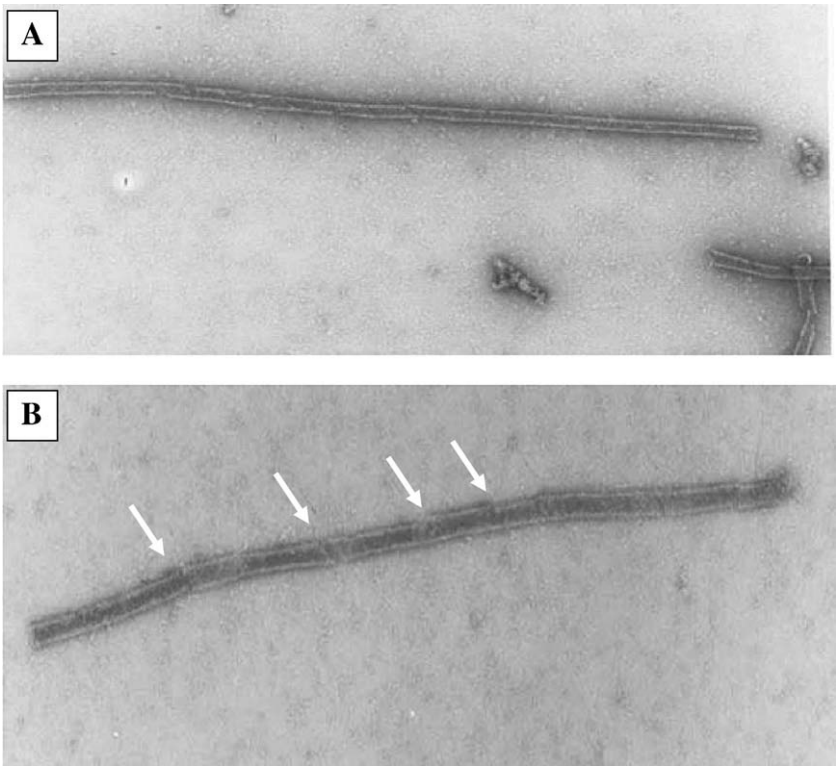

Fig. 2. Electron micrograph of the reassociation of dissociated RvH1. Purified RvH1 was obtained by ion-exchange chromatography [28] after overnight dialysis against 50 mM Tris/HCl buffer, pH 9.6. Reassociation was performed in A) 50 mM Tris/HCl buffer, pH 7.0, containing 50 mM $CaCl_2$ and $MgCl_2$ within 3 days and twisted ribbon helical tubules, yet not fully annealed were produced; (B) 100 mM $CaCl_2$ and $MgCl_2$ after dialysis of RvH1 for 3 days very nice tubules and also multidecamers can occur. Negative staining with 1% uranyl acetate was performed. The scale bar indicates 100 nm.

Table 1
Effective thermodynamic parameters of thermal denaturation of *Rapana venosa* hemocyanin in three structural forms: RvH, RvH1 and RvH2

pH	T_m (°C)		ΔT (°C)		Area (relative)		ΔH_{eff} (kcal/mol)		$\Delta H_{eff,tot}$ (kcal/mol)
	1	2	1	2	1	2	1	2	
A. RvH intact									
2.5	46.5	34.1	22.8	11.7	−1.14	−0.19	−33.9	−63.8	−97.8
3.0	57.0	41.1	20.0	19.3	−0.48	−1.36	−57.0	−41.8	−101.8
4.0	38.4	47.8	9.6	25.1	−0.22	−1.94	−30.6	−32.6	−63.2
5.0	56.4	39.9	31.5	22.4	−1.99	−1.41	−19.5	−32.8	−50.2
6.5	55.9	50.2	32.8	23.7	−1.69	−1.10	−26.1	−35.0	−61.1
7.0	55.1	34.1	27.2	7.3	−2.60	−0.11	−31.4	−103.1	−134.5
8.0	54.1	35.4	29.2	11.8	−2.10	−0.20	−29.0	−95.1	−124.1
9.0	33.3	52.9	11.5	27.2	−0.13	−2.17	−64.4	−31.0	−95.4
10.0	34.1	53.6	12.7	25.5	−0.20	−1.90	−58.9	−33.2	−92.1
11.0	37.3	54.2	12.7	25.5	−0.20	−1.95	−59.3	−33.3	−92.6
12.0	–	–	–	–	–	–	–	–	–
B. RvH1									
2.5	35.7	55.3	9.2	26.3	−0.07	−1.73	−82.5	−32.5	−115.0
3.0	36.7	56.7	8.6	24.0	−0.08	−1.43	−84.4	−36.0	−120.4
4.0	37.2	56.1	10.5	24.6	−0.28	−1.89	−73.1	−34.9	−108.0
5.0	38.1	59.1	15.1	23.2	−0.58	−1.75	−50.7	−37.6	−88.3
6.0	35.9	57.1	12.9	27.0	−0.50	−2.25	−58.5	−32.0	−90.5
7.0	40.4	60.4	13.7	19.8	−0.60	−1.20	−56.1	−44.4	−100.5
8.0	55.6	61.8	9.1	23.2	−0.53	−2.41	−94.1	−38.3	−132.4
9.0	53.8	61.6	7.0	23.9	−0.12	−2.41	−120.8	−37.1	−158.0
10.0	71.2	57.4	15.0	17.3	−1.40	−1.90	−62.4	−50.1	−112.5
11.0	44.2	64.3	17.0	21.1	−0.57	−3.20	−47.0	−42.8	−89.8
12.0	–	–	–	–	–	–	–	–	–
C. RvH2									
2.5	42.5	58.7	13.5	18.9	−0.53	−1.38	−58.3	−46.1	−104.4
3.0	41.7	60.1	11.0	19.1	−0.41	−1.30	−71.6	−46.0	−117.6
4.0	38.0	60.0	17.6	22.8	−0.38	−1.38	−43.5	−38.4	−81.9
5.0	41.3	61.9	10.8	16.1	−0.37	−0.86	−72.2	−55.1	−127.3
6.0	39.2	62.2	12.0	16.2	−0.38	−0.80	−64.9	−55.1	−120.0
7.0	48.1	60.6	11.6	16.6	−0.19	−0.10	−70.3	−53.0	−123.3
8.0	55.6	71.2	17.9	11.4	−1.04	−0.36	−47.8	−82.0	−129.8
9.0	64.8	47.9	18.1	24.7	−0.50	−1.24	−50.0	−33.3	−83.3
10.0	40.6	60.0	13.2	20.4	−0.46	−1.27	−59.0	−43.0	−102.0
11.0	44.9	63.2	18.4	18.0	−0.81	−0.86	−43.6	−49.7	−93.2
12.0	39.7	62.4	16.4	19.6	−0.88	−1.20	−47.3	−45.4	−92.7

the curves it is clear that they are composed by two or more components and represent complex temperature transitions (Fig. 4A), which is also visible for the isolated subunits (Fig. 4B and C). Even smooth pH dependence influences specific T-dependent stability, as shown in a number of give curves, which have different features to those others in the same family. Lastly, the two subunits have different sets of $[\theta]_{222}(T, \text{pH})$ data as shown by comparing Fig. 4B and C.

3.4. Influence of pH on dichroic amplitude at 222 nm (at different temperatures)

The $[\theta]_{222}$/pH plot at different temperatures shows remarkable differences comparing those of native RvH with those its subunits (Fig. 5A, B, and C). For native RvH, the $[\theta]_{222}$/pH plots represent a set of smooth and partially "bell shaped" curves with maxima between pH 5–8 and non-symmetric acidic and alkaline extremes, but without any obvious sigmoid feature at extreme pH. In the alkaline part (pH 8–12), relative changes are too small and non-cooperative (within a wide pH interval), indicating that alkaline denaturation cannot be achieved as reversible process. For isolated subunits the behaviour is different: for the complete set of the pH curves at different temperatures, suggesting a number of pH-dependent processes with well-expressed maxima of $[\theta]_{222}$(pH), for the full set of isotherms at pH ~ 8. The complete set of curves can be deconvoluted as the sum of six pH-dependent processes (Fig. 5B). The same should be expressed by Fig. 5A, C, but the processes are overlapped and not resolved. Each will have its own apparent $pK_{a,i}$, with a specific $pK_{a,i}(T)$ dependence, i.e. group enthalpy of ionization. Because there is a large difference of $\Delta H_{ion,i}$ these values are indicative of the ionized nature of the groups responsible for any given local $[\theta]_{222}$(pH) change.

3.4.1. Subunit RvH1

As shown in Fig. 5B (standard conditions, at 25 °C) acid denaturation ($pH_{d,a}$) is at pH 3.6 and alkaline denaturation ($pH_{d,b}$) at pH 11.0. The acid curves show a small T dependence, which is higher for alkaline denaturation. In the native state, at pH ~ 5.3 and 7.0, there are ionizations (due to carboxylates and imidazoles), causing a proton deficit increasing the apparent $[\theta]_{222}$. The presence of a slight peak in the pH range (7.5–9.0) indicates the presence of two ionization processes, with an opposing influence on left (L) and right (R) limbs of $[\theta]_{222}$(pH), respectively ($pK_{a,L}$ 7.8 and $pK_{a,R}$ 8.7). In all respects, $pK_{a,L}$ have greater temperature dependence than $pK_{a,R}$.

3.4.2. Subunit RvH2

The behaviour of the second subunit (Fig. 5C) is analogous but not identical to RvH1: under standard conditions of acid denaturation in the range pH 2–4, denaturation is not well-resolved or shifted at lower pHs and neither is alkaline denaturation (absence of drastic drop of $[\theta]_{222}$, even at pH 12). Also, at neutral pH (6.5–8.5) a wide plateau is present. With increasing temperature of 45–50 °C the characters of the $[\theta]_{222}$(pH) curves are changed and they become similar to the corresponding $[\theta]_{222}$ (pH) curves of subunit RvH1, even showing a slight peak at pH 7 (compare Fig. 5B and C). Comparing the two sets of curves if becomes obvious that at low temperatures (25–45 °C), both are less pH-dependent compared to higher temperatures (50 °C and above).

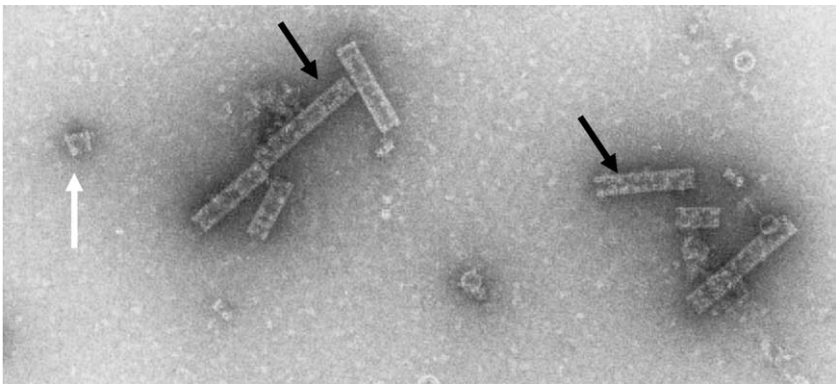

Fig. 3. Electron micrograph of reassociated RvH2 from a dissociated sample performed at pH 9.6. Purified RvH2, dissociated into subunits, produced didecamers (white arrowhead), short multidecamers (black arrowheads) with some remaining subunits after dialysis for 3 days against stabilizing buffer, pH 7.0, containing 50 mM $CaCl_2$, 2 mM $MgCl_2$. Complete reassociation of RvH2 into stable decamers does not occur under these conditions.

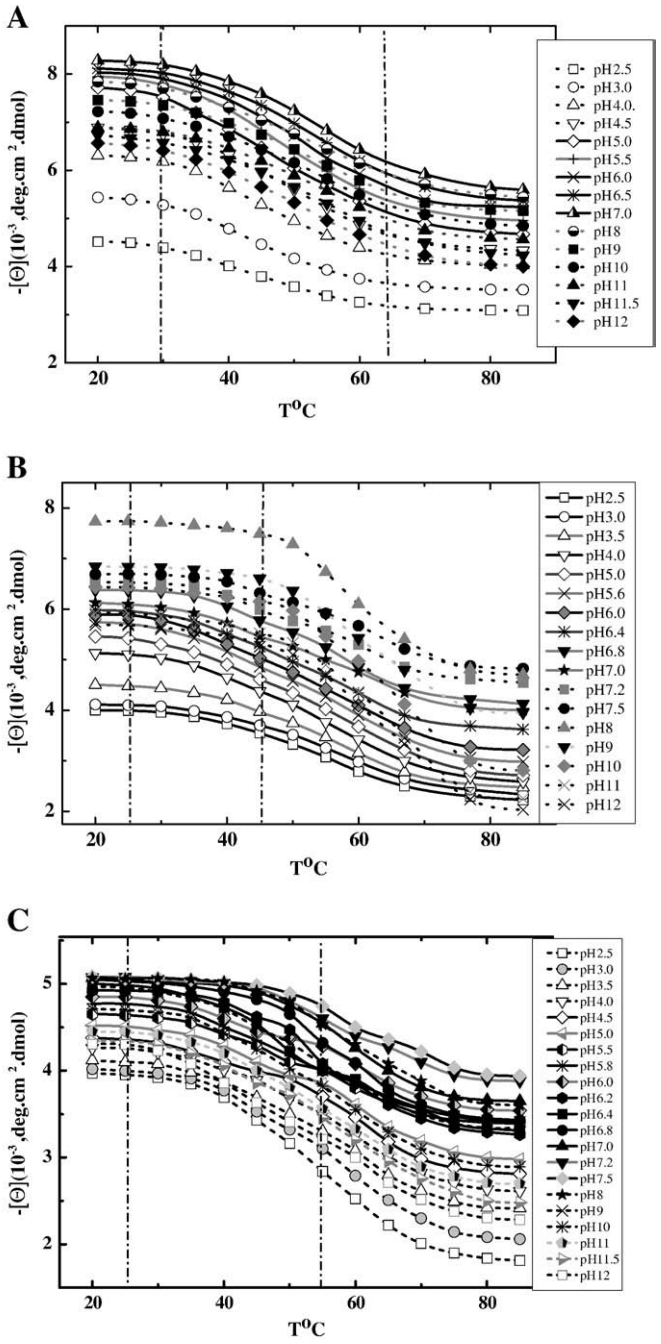

Fig. 4. Influence of temperature on circular dichroism spectra at different pH values. The *T*-induced changes are shown over a wide temperature interval (25–85 °C). The curves $[\theta]_{222}(T)$ are shown for native Hc (RvH) (A) and for isolated subunits RvH1 (B) and RvH2 (C). Curves considered to be "reversible" are indicated within 2 vertical dashed lines.

3.5. $[\theta]_{222}(T)$–$[\theta]_{222}(pH)$ functions — reversibility

Because of the large set of experimental points in the *T*–pH grid of $[\theta]_{222}$, we take "dissections" at a given temperature for discrete pH values and *vice versa* (at given pH for corresponding temperatures) and have converted the data to a new pair of data sets. If the principle of thermodynamic independence of the denaturation state from the way of its achievement is correct, then we should obtain the same results. We accept that extension of the relative identity (in %) is a measure and criterion of reversibility. The results from this "morphing" for native Hc RvH and subunits RvH1 and RvH2 are shown in Fig. 6A, B, C, respectively. The lines connect *T*–pH points with equal reversibility (%) as 100 (1), 96 (2), 92 (3), 88 (4) and 80 [5]. We propose that this "phase portrait" for reversibility in pH–*T* perturbations for given objects is valid. As is shown in all cases, the reversibility at 25 °C is low above pH 6 i.e. the systems are irreversible. Increasing temperature and within the *T* range 35–45 °C the reversibility increases and "opens a window" within the range of pH 4–6. At temperatures above 50 °C, the three protein systems become different with respect to their reversibility at extreme temperatures and corresponding pH regions. Both RvH subunits display a markedly different behaviour at pH 7 and around 60 °C. In general, subunit RvH1 is less reversibly denatured than subunit RvH2 and it shows larger changes at pH 7 within 50–60 °C.

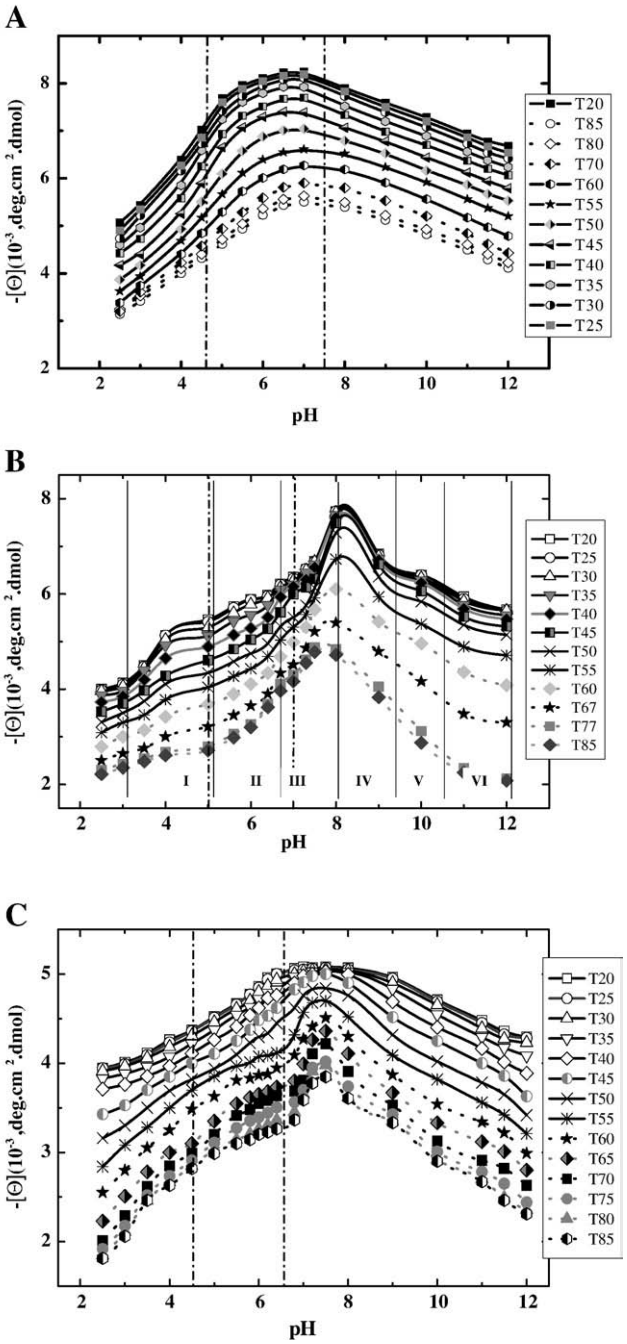

Fig. 5. Influence of pH on $[\theta]_{222}$ of RvH, RvH1 and RvH2 at different temperatures. Note the difference $[\theta]_{222}$(pH) between native Hc RvH (A) and its purified subunits RvH1 (B) and RvH2 (C) with respect to pH (over a wide pH range). Curves considered to be "reversible" are indicated within vertical dashed lines.

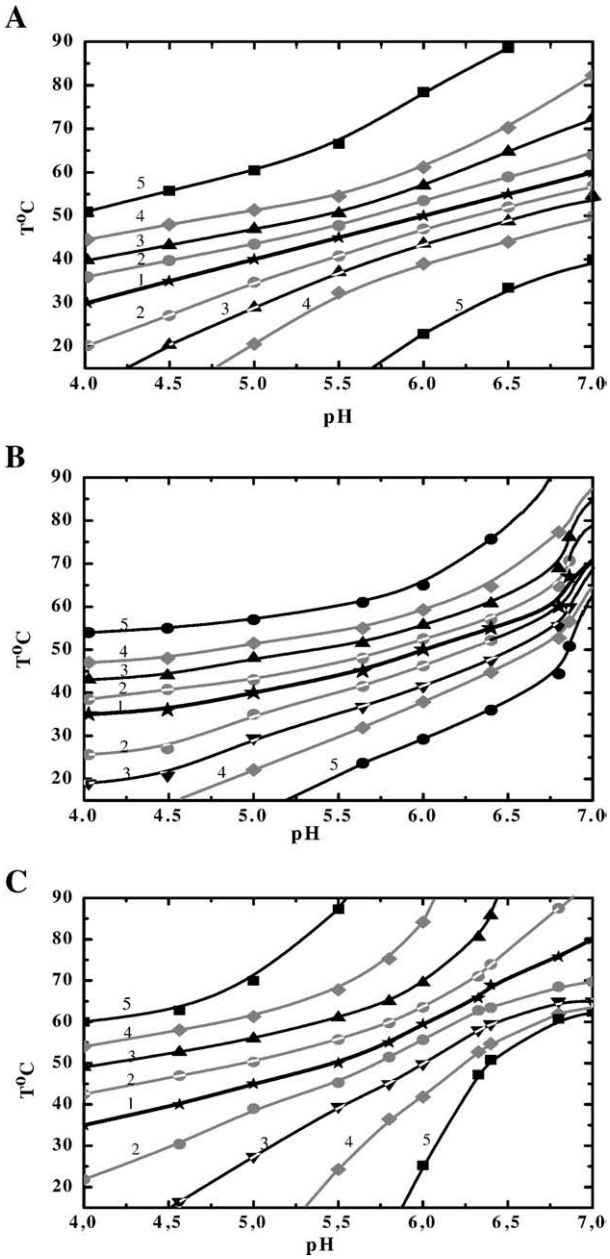

Fig. 6. *T*–pH "phase diagram". Curves were obtained by $[\theta]_{222}(T)$–$[\theta]_{222}$(pH) functions showing their denaturation reversibilities for native Hc RvH(A), subunits RvH1(B), and RvH2(C). The lines connect *T*–pH points with equal reversibility (%) as 100 (1), 96 (2), 92 (3), 88 (4) and 80 (5).

3.6. T–pH "phase diagram" (a two-domain system)

Using different techniques (two-component *T*-transition equations, graphical and numerical differentiation and Gaussian separation–deconvolution) the *T*-transition curves at different pH for each of three RvH systems were analyzed and the parameters (Table 1) and thermodynamic functions were obtained. Representative results are presented in Figs. 4–6.

The overview shown in Table 1 indicates the high and relatively pH-independent effective enthalpy of thermal denaturation, which is very similar for all three systems: the two isolated and purified subunits and the native RvH (which contains RvH1 and RvH2 subunits). The second feature is the presence as minima of two "thermodynamic domains" — all structures behave as the sum of two parts with different thermodynamic properties. Their separation is difficult because they overlap in both, the *T* and pH scales and are not stable.

Using reversibility analysis, the curves shown in Figs. 4 and 5 are considered to be "reversible", shown by the solid-line curves in the undependable (*T* or pH) intervals, marked by the vertical dashed lines. Part 2 from the curves is considered to be dependable (*T* or pH) intervals.

4. Discussion

In the literature there are a limited number of papers directed towards the biophysical and structural understanding of hemocyanin stability and function. This is not surprising because of the complexity of gastropod hemocyanin structure, created from multiple subunits each containing seven or eight similar, but not identical, functional units. Hydrodynamic parameters of *Rapana* hemocyanin have previously been determined by dynamic light scattering, which allowed characterization of conformational changes [21]. Also, the thermal denaturation of *Rapana* hemocyanin was studied by scanning calorimetry, using different biological buffers to investigate buffer effects. Although these authors showed up to 55% conformation/denaturation reversibility, several parameters such as enthalpy, melting temperature, C_p were calculated [22]. However, the mechanism of thermal denaturation of *Rapana* hemocyanin is of a complicated character and the process of thermal unfolding is irreversible. Thus, neither real thermodynamic data nor structurally related activation parameters could be obtained. This limited background was the reason for a detailed molecular analysis presented in this report.

Studies on the stability and reassociation behaviour of the whole molecule of *R. venosa* hemocyanin and the structural subunits in stabilizing buffer (SB), pH 7.0, were performed in the presence of different concentrations of Ca^{2+} and Mg^{2+} ions and different pH and assessed using electron microscopy. Purified (dissociated) structural subunits RvH1 and RvH2 showed a different reassociation behaviour compared to the mixed subunits produced from the native molecules. Also the behaviour of RvH2 differs from that of RvH1, but similarly depends on pH and concentration of Ca^{2+} and Mg^{2+} ions. The dissociated RvH1 in 50 mM Tris/HCl buffer (pH 9.6) after a period of 3 days dialysis against 50 mM Tris/HCl buffer, (pH 7.0) containing 50 or 100 mM $CaCl_2$ and $MgCl_2$, reassociated as tubules, while RvH2 reassociated into short multidecamers, tubules and didecamers. The stability of the reassociated RvH1 and RvH2 was pH-dependant and after dialysis against 50 mM Tris/HCl buffer, pH 8.6, containing 100 mM $CaCl_2$ and $MgCl_2$, the length of the RvH1 helical tubules become shorter. It was found that the prolongation of the dialysis for 1 week leads to their dissociation into short helices [11]. Mostly short multidecamers, didecamers, decamers and subunits were observed after increasing the pH to 9.2 [11].

Tubular polymers were produced not only after reassociation of RvH1 subunits, in presence of 100 mM $CaCl_2$ and $MgCl_2$ [11], but also from subunits of KLH [18], HtH and *H. pomatia* Hc [30,31]. The speed of reformation for RvH1, KLH and HtH subunits was more rapid at concentrations of 100 mM $CaCl_2$ and $MgCl_2$ than at 20 and 50 mM. For the RvH1 subunit the situation after reassociation in the presence of calcium and magnesium ions parallels more closely to KLH2 and HtH2 than to RvH2, KLH1 and HtH1 [11,29].

RvH1 and RvH2 differ not only in their reassociation behaviour, but also the tubules of RvH1 showed a different stability at higher pH values compared to RvH2. RvH2 multidecamers are less stable than those of RvH1 [11].

T transitions — The range of $[\theta]_{222}$ *T*-changes are too wide to be a single transition (Fig. 4A, B and C). Because of lack of direct steps, the results probably show a number of transitions and they overlap greatly on the T scale. Because all *T*-transition curves for the three hemocyanin species over a wide pH range are very similar, it is reasonable to suggest that in solution the isolated subunits behave as multimers and resemble native RvH. The relatively small changes of initial $[\theta]_{222}$ at high temperatures indicate that many secondary structure elements are preserved, especially at neutral pH and even at

extreme high temperatures. Thus we have not detected *T*-dependent unfolding and probably even at temperatures above 90 °C the proteins retain a "globule state".

pH transitions (acid and alkaline denaturation) are poorly presented in all the extremes within the data sets of total RvH and its two subunits and can be accounted for by an increased stability due to quaternary structure. This is supported by comparing the data from native RvH and its two subunits. RvH is more stable, especially in the alkaline region. If the "peak" shown in Fig. 5B for subunit RvH1 represents a pH-dependent removal of Cu ions from the protein, the absence of such a "peak" in Fig. 5C at temperatures 20–40 °C could lead to the conclusion that subunit RvH2 is stabilized by a currently unknown additional "factor". This factor should be non-ionic in nature and we could suggest that carbohydrate moieties are involved. An increase in temperature from 20–45 °C may lead to a conformational change of the oligosaccharide residues.

pH–T phase diagrams — Reversibility of pH–*T* denaturation is the base paradigm of protein self-organization and the applicability of reversible thermodynamics approach can be used for evaluation of its stability. After Anfinsen et al. [32], this paradigm was experimentally proven many times (since 1967 [33,34]) and adjusted with validity of the simple two-state model [26]. Of course, the reality is much more complex; many more complicated schemes were described. However, to the best our knowledge, at present time there exist no experimental data showing the degree of irreversibility of a protein system, performed in this report with our pH–*T* diagrams (Fig. 6A, B, C), which are typical "phase portraits" for each of three similar, but not identical objects. For the three objects, the 100–80% reversibility is possible only in acidic pH range. The multimeric intact Hc RvH structure (Fig. 6C) has a small interval of partial reversibility close to pH 4 and big perturbance in the region of pH 7. The subunits show higher reversibility at 25 °C within pH intervals 4.1–4.7 and 4.2–5.3 for both subunits RvH1 and RvH2, respectively (Fig. 6A and B). A further main conclusion is, that probably Hc chains agglomerate at weak acidic pH which is typical for gastropod hemolymph when most of carboxylates are protonated, and thus the repulsive interactions are diminished.

Acknowledgements

This work was supported by a research grant by NATO (Collaborative Programmes Section, CBP.EAP.CLG 981 969), DFG GZ:436 BUL 113/149/0-1 (Deutsche Forschungsgemeinschaft), CNR (Italy), Ministry of Sciences and Education by grants: DAAD-9/2007 (Germany); (VU-L-310/07, X-1310). Dr. P. Dolashka-Angelova would like to thank DFG and DAAD for granting a scholarship.

References

[1] J. Markl, Evolution and function of structurally diverse subunits in the respiratory protein hemocyanin from arthropods, Biol. Bull. (Woods Hole) 171 (1986) 90–115.
[2] K.E. Van Holde, K.I. Miller, Hemocyanins, Adv. Protein. Chem 47 (1995) 1–81.
[3] K. Streit, D. Jackson, B.M. Degnan, B. Lieb, Developmental expression of two *Haliotis asinina* hemocyanin isoforms, Differentiation 73 (2005) 341–349.
[4] M.E. Cuff, K.I. Miller, K.E. van Holde, W.A. Hendrickson, Crystal structure of a functional unit from *Octopus* hemocyanin, J. Mol. Biol 278 (1998) 855–870.
[5] W. Gebauer, J.R. Harris, H. Heid, M. Süling, R. Hillenbrand, S. Söhngen, A. Wegener-Strake, J. Markl, Quaternary structure, subunits and domain patterns of two discrete forms of keyhole limpet hemocyanin: KLH1 and KLH2, Zoology 98 (1994) 51–68.
[6] B. Lieb, B. Altenhein, J. Mark, The sequence of a gastropod hemocyanin (HtH1 from *Haliotis tuberculata*), J. Biol. Chem 275 (2000) 5675–5681.
[7] P. Dolashka-Angelova, M. Schick, S. Stoeva, W. Voelter, Isolation and partial characterization of the N-terminal functional unit of subunit RtH_1 from *Rapana thomasiana* grosse hemocyanin, Int. J. Biochem. & Cell Biology 32 (2000) 529–538.
[8] K.E. Van Holde, K. Miller, E. Schabtach, L. Libertini, Assembly of *Octopus dofleini* hemocyanin. A study of the kinetics by sedimentation, light scattering and electron microscopy, J. Mol. Biol 217 (1991) 307–321.
[9] C.F. Bonafe, J.R.V. Araujo, J.L. Silva, Intermediate states of assembly in the dissociation of gastropod hemocyanin by hydrostatic pressure, Biochemistry 33 (1994) 2651–2660.
[10] S.M. Söhngen, A. Stahlman, J.B. Harris, S.A. Müller, A. Engel, J. Markl, Mass determination, subunit organization, and control of oligomerization states of keyhole limpet hemocyanin (KLH), Eur. J. Biochem 248 (1997) 602–614.
[11] P. Dolashka-Angelova, H. Schwarz, A. Dolashki, M. Beltramini, B. Salvato, M. Schick, M. Saeed, W. Voelter, Characterization of the reassociation and oligomeric stability of *Rapana venosa* hemocyanin (RvH) and its structural subunits, Biochim. Biophys. Acta 1646 (1–2) (2003) 77–85.
[12] P. Dolashka, N. Genov, K. Parvanova, W. Voelter, M. Geiger, S. Stoeva, *Rapana thomasiana* grosse (gastropoda) haemocyanin: spectroscopic studies of the structure in solution and the conformational stability of the native protein and its structural subunits, Biochem. J. 315 (1996) 139–144.
[13] R. Hristova, P. Dolashka, S. Stoeva, W. Voelter, B. Salvato, N. Genov, Spectroscopic properties and stability of hemocyanins, Spectrochim. Acta Part A 53 (1997) 471–478.
[14] P. Dolashka-Angelova, R. Hristova, S. Stoeva, W. Voelter, Spectroscopic properties of *Carcinus aestuarii* hemocyanin and its structural subunits, Spectrochim. Acta Part A 55 (1999) 2927–2934.
[15] P. Dolashka-Angelova, S. Stoeva, R. Hristova, J. Schuetz, M. Beltramini, B. Salvato, H. Schwartz, W. Voelter, Structural organization of hemocyanin from lobster *Homarus americanus* and spectroscopic studies of the native protein and structural subunits, Current Topics in Peptide & Prot. Res 3 (1999) 19–36.
[16] P. Dolashka-Angelova, S. Stoeva, R. Hristova, J. Schuetz, W. Voelter, Structural and spectroscopic studies of the native hemocyanin from *Maia squinado* and its structural subunits, Spectrochim. Acta Part A 56 (2000) 1985–1999.
[17] P. Dolashka-Angelova, A. Dolashki, S. Stevanovic, R. Hristova, B. Atanasov, P. Nikolov, W. Voelter, Structure and stability of arthropodan hemocyanin *Limulus polyphemus*, Spectrochim. Acta Part A 61 (6) (2005) 1207–1217.
[18] J. Schütz, P. Dolashka-Angelova, R. Abrashev, P. Nikolov, W. Voelter, Isolation and spectroscopic characterization of the structural subunits of keyhole limpet hemocyanin, Biochim. Biophys. Acta 1546 (2001) 325–336.
[19] S. Stoeva, P. Dolashka, N. Genov, W. Voelter, Domain structure of the *Rapana thomasiana* (Gastropod) hemocyanin, GIT Special "Prof. Bayer" (1997) 75–79.
[20] S. Stoeva, P. Dolashka, K. Pervanova, N. Genov, W. Voelter, Multidomain structure of the *Rapana thomasiana* (Gastropod) hemocyanin structural subunit RHSS1, Comp. Biochem. Physiol. 118B, 4 (1997) 927–934.
[21] D. Georgieva, D. Schwark, P. Nikolov, K. Idakieva, K. Parvanova, K. Dierks, N. Genov, C. Betzel, Conformational states of the *Rapana thomasiana* hemocyanin and its substructures studied by dynamic light scattering and time-resolved fluorescence spectroscopy, Biophys J 88 (2005) 1276–1282.
[22] K. Idakieva, K. Parvanova, S. Todinova, Different scanning calorimetry of irreversible denaturation of *Rapana thomasiana* (marine snail, Gastropod) hemocyanin, Bioch. Biophys. Acta 1748 (2005) 50–56.
[23] M. Guzman-Casado, A. Parody-Morreale, P.L. Mateo, J.M. Sanchez-Ruiz, Differential scanning calorimetry of lobster haemocyanin, Eur. J. Biochem 188 (1990) 181–185.
[24] R. Voit, G. Feldmaier-Fuchs, T. Schweikardt, H. Decker, T. Burmester, Complete sequence of the 24-mer hemocyanin of the tarantula *Eurypelma californicum*. Structure and intramolecular evolution of the subunits, J. Biol. Chem. 15 275 (50) (2000) 39339–39344.
[25] Y. Liu, J.M. Sturtevant, The observed change in heat capacity accompanying the thermal unfolding of proteins depends on the composition of the solution and on the method employed to change the temperature of unfolding, Biochemistry 35 (1996) 3059–3062.
[26] P.L. Privalov, N.N. Khechinashvili, B.P. Atanasov, Thermodynamic analysis of thermal transitions of globular proteins. calorimetric study of chymotrypsinogen, ribonuclease and myoglobin, Biopolymers 10 (1971) 1865–1890.
[27] P.L. Privalov, S.J. Gill, Stability of protein structure and hydrophobic interaction, Adv. Protein Chem 39 (1988) 191–234.
[28] P. Dolashka-Angelova, S. Stefanovic, A. Dolashki, B. Devreese, B. Tzvetkova, W. Voelter, J. Van Beeumen, B. Salvato, A challenging insight on the structural unit 1 of molluscan *Rapana venosa* hemocyanin, Arch. Biochem. Biophys 1 459 (2007) 50–58.
[29] J.R. Harris, D. Scheffler, W. Gebauer, R. Lehnert, J. Markl, *Haliotis tuberculata* hemocyanin (HtH): analysis of oligomeric stability of HtH1 and HtH2, and comparison with keyhole limpet hemocyanin KLH1 and KLH2, Micron 31 (2000) 613–622.
[30] B. Lieb, B. Altenhein, J. Markl, A. Vincent, E. van Olden, K.E. van Holde, K.I. Miller, Structures of two molluscan hemocyanin genes: significance for gene evolution, Proc. Natl. Acad. Sci. USA 98 (2001) 4546–12455.
[31] J.R. Harris, J. Markl, Keyhole limpet hemocyanin (KLH): a biomedical review, Micron 30 (1999) 597–623.
[32] D. Givol, F. De Lorenzo, A. Goldberger, C.B. Anfinsen, Disulfide Interchange and the three-dimensional structure of proteins, Proc. Natl. Acad. Sci. USA 53 (1965) 676-684.
[33] J. Hermans, G. Acampora, Reversible denaturation of sperm whale myoglobin. I. Dependence on temperature, pH and composition; II. Thermodynamic analysis, J. Amer. Chem. Soc 89 (1967) 1543–1552.
[34] B.P. Atanasov, S. Mitova, On the reversibility of thermal denaturation of *Delphinus delphis* ferri myoglobin derivatives, Biophim. Biophys. Acta 214 (1970) 69–82.